Einstein–de Haas phase shifts in surface acoustic waves

Shoma Tateno, Yuki Kurimune, Mamoru Matsuo, Kazuto Yamanoi, and Yukio Nozaki

Phys. Rev. B **104**, L020404 — Published 9 July 2021

DOI: 10.1103/PhysRevB.104.L020404

Einstein-de Haas phase shifts in surface acoustic waves

Shoma Tateno[1], Yuki Kurimune[1], Mamoru Matsuo[2,3,4], Kazuto Yamanoi[1] and Yukio Nozaki [1,5]
[1] *Department of Physics, Keio University, Yokohama 223-8522, Japan*
[2] *Kavli Institute for Theoretical Sciences, University of Chinese Academy of Sciences, No. 3, Nanyitiao, Zhongguancun, Haidian District, Beijing 100190, China.*
[3] *RIKEN Center for Emergent Matter Science (CEMS), Wako, Saitama 351-0198, Japan.*
[4] *Advanced Science Research Center, Japan Atomic Energy Agency, Tokai, 319-1195, Japan.*
[5] *Center for Spintronics Research Network, Keio University, Yokohama 223-8522, Japan*
(Dated: June 22, 2021)

We demonstrate the phase shift of the Rayleigh-type surface acoustic wave (RSAW) in a ferromagnetic $Ni_{79}Fe_{21}$ film based on the gyromagnetic Einstein-de Haas (EdH) torque that can be attributed to the back action of spin-wave excitation. The EdH torque modulates the transverse velocity of the bulk acoustic wave that causes the bipolar phase shift of RSAW. When compared with a magnetoelastic torque, the phase shift can be more prominently enhanced by increasing the frequency. The gyromagnetic torque in the RSAW paves the way for controlling spin-mechatronics devices without magnetoelastic torque which is specific to a certain material.

Einstein-de Haas (EdH) effect is a fundamental gyromagnetic phenomenon, based on which the conversion of angular momentum from microscopic spin to mechanical rotation can be clearly observed [1]. The EdH effect is a spin-dependent inertial phenomenon owing to the spin-vorticity coupling (SVC), originating from the general relativistic Dirac equation [2–6]. In addition, the spin-orbit interaction (SOI), which is based on special relativity, can also convert the angular momentum similarly. Indeed, acoustically driven ferromagnetic resonance has been successfully demonstrated using magnetoelastic coupling [7–10] and magneto-rotation coupling [11]. From both fundamental and application viewpoints, it is important to understand the general and special relativity effects caused by temporally and spatially nonuniform rotation of ferromagnetic lattice systems. Especially, the gyromagnetic effect in a ferromagnetic metal is an interesting research subject because the SVC-driven phenomenon can be experimentally investigated in strongly correlated solids. However, there are few studies on the gyromagnetic effect in solids because of its tiny signal generated by kHz order rotational motion. Generally, such a tiny EdH torque has been detected based on mechanical resonance. Increasing the resonant frequency of the mechanical resonator, i.e., decreasing the mass moment of inertia, is essential for improving the detectable EdH torque. The resonant frequency of the mechanical resonator can be increased because of recent developments in the microfabrication technology for micro-electro-mechanical-systems (MEMSs). Using such MEMS resonators, the EdH mechanical force owing to the spin-wave current [12] and the EdH torque produced by a radiofrequency magnetic field [13] have been successfully observed.

In case of the bulk acoustic wave (BAW) excitation associated with ultrafast laser-induced demagnetization, alternating demonstration of the EdH effect has been realized without using a mechanical resonator [14]. In the time-resolved X-ray diffraction experiment, an impulsive transverse BAW can be observed within 200 femtoseconds after ultrafast demagnetization because of intense photoexcitation. This result indicated that angular momentum can be transferred between spin and lattice systems in a subpicosecond time scale. Furthermore, the efficiency of angular momentum conversion between spin and lattice systems became approximately 80%. The EdH effect is a promising candidate to ensure the ultrafast and energy-efficient operation of spin mechatronics devices.

In this Letter, we successfully demonstrated the phase shift of the Rayleigh-type surface acoustic wave (RSAW) based on the EdH effect in a ferromagnetic $Ni_{79}Fe_{21}$ thin film . The RSAW is known as the collective harmonic oscillation of atomic lattice in elastic materials. Recently, the RSAW has been widely investigated for spin current generation [5, 15–18], field sensing [19], acoustic rectification [11, 20–27], and magnetization switching [28, 29]. When the RSAW propagates through a ferromagnetic thin film, the gyromagnetic spin-wave resonance (SWR) is excited owing to the Barnett effect [31, 32] which enables the transformation from the mechanical angular momentum of RSAW to the magnetic angular momentum. In the previous study [30], the SWR amplitude has been evaluated from a gyromagnetic attenuation of RSAW according to an energy conservation between RSAW and SW. It is noted that the gyromagnetic effect in RSAW is reciprocal as can be inferred from the EdH and Barnett effects originally observed in an iron rigid body [1, 31, 32]. Namely, we can also attribute the attenuation of the RSAW to the EdH effect caused by the SWR excitation. Recently, the back action of the magnetoelastic effect in case of RSAW propagating through a ferromagnetic thin film has been theoretically predicted [33]. We develop an analytic model that extends this theory to include the contributions of EdH torque to elastic motion and find that the additional stress that can be

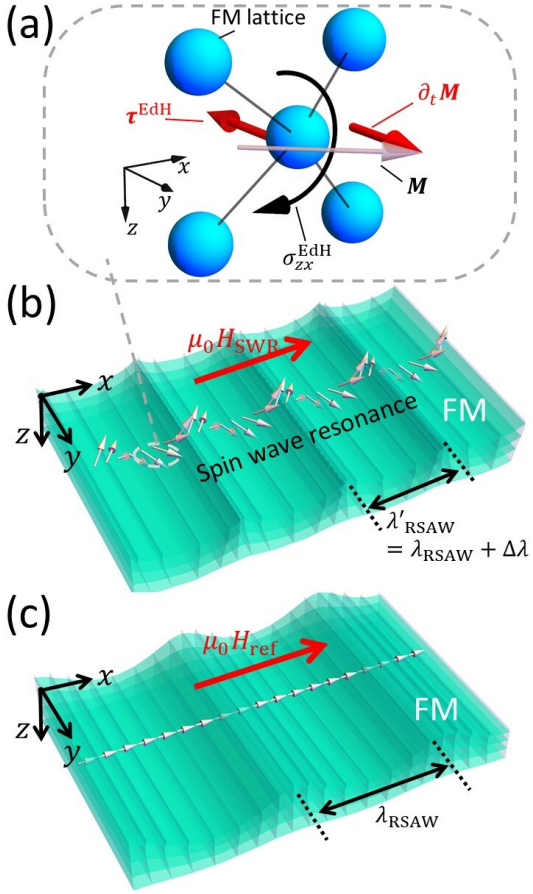

FIG. 1. (a) Schematic of the stress component $\sigma_{zx}^{\mathrm{EdH}}$ generated by the EdH effect. The direction of EdH torque is opposite to the temporal derivative of magnetization $\partial_t \boldsymbol{M}$. Illustration of RSAW propagating through the FM thin film (b) with and (c) without the excitation of SWR. An external field is applied parallel to the wave vector of the RSAW so that MSBVW is excited. The wavelength of the RSAW λ_{RSAW} is modulated by $\Delta\lambda$ owing to the EdH effect in FM.

attributed to the EdH effect (shown in Fig. 1(a)) modulates only the transverse sound velocity c_{t} of the bulk acoustic waves, although the longitudinal sound velocity c_{l} does not change at all. As a consequence, the RSAW velocity c_{R}, which depends on c_{t} and c_{l}, is modulated by the EdH effect, resulting in a change in the wavelength, as schematically shown in Figs. 1(b) and 1(c). Thus, through our phase-sensitive measurement using a vector network analyzer (VNA), the phase shift could be successfully detected, the magnitude and frequency variations of which are consistent with our analytical predictions.

Figure 2 schematically presents the setup used for measuring the EdH phase shifts in the RSAW propagating through a ferromagnetic $Ni_{79}Fe_{21}$ film. A pair of interdigital transducers (IDTs) comprising Ti(3)/Au(30) is fabricated via electron beam lithography and electron beam evaporation on a piezoelectric $LiNbO_3$ substrate.

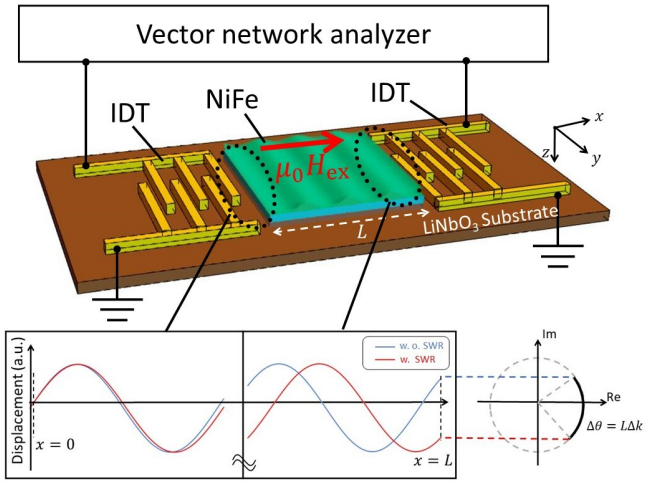

FIG. 2. Experimental setup for measuring the phase shift $\Delta\theta$ of the RSAW because of the EdH effect. A pair of IDTs and $Ni_{79}Fe_{21}$ film is deposited on the $LiNbO_3$ substrate. The external field $\mu_0 H_{\mathrm{ex}}$ is applied along the RSAW propagation direction.

The numbers in parentheses indicate the layer thickness in nanometers. The nominal values for width and spacing distance of the finger electrode of IDT are varied from 500 to 750 nm which leads to a change in the RSAW frequency from 1.9 to 1.3 GHz. The wavelength of RSAW originally excited by the IDT is 4 times as long as the finger width. Further, the edge distance between a pair of IDTs is 461 μm. The $Ni_{79}Fe_{21}(20)$ film with a lateral size of 400 × 400 μm^2 is sputtered between a pair of IDTs. When an alternating current (AC) voltage is applied to one of the IDTs, a periodical stress is produced in the $LiNbO_3$ substrate below the IDT via the inverse piezoelectric effect followed by the propagation of RSAW. The propagated RSAW is detected by the other IDT based on the direct piezoelectric effect. In the experiment, the amplitude and phase modulation of the RSAW are examined based on the measurement of S_{21}. If the RSAW velocity is modulated via EdH effect in FM, the phase shift of the propagated RSAW appears as schematically shown in Fig. 2, where the FM has spread between $x = 0$ and L. In addition, an external field $\mu_0 H_{\mathrm{ex}}$ is applied along the RSAW propagation direction, ensuring excitation of the magnetostatic backward volume wave (MSBVW). The amplitude of $\mu_0 H_{\mathrm{ex}}$ is swept from -10 to 10 mT. We perform the time gating signal processing for the measured S_{21} to exclude the signal that can be attributed to the leakage of electromagnetic field from the IDT [15, 16, 21, 30]. The phase shift of RSAW has been evaluated at $x = L$ based on the values of S_{21} in case of different external fields as follows:

$$\Delta\theta(H) = \arg\left(\frac{S_{21}(f_{\mathrm{RSAW}}, H)}{S_{21}(f_{\mathrm{RSAW}}, H_{\mathrm{ref}})}\right), \qquad (1)$$

where f_{RSAW} is the frequency at which RSAW is excited

and $H_{\rm ref}$ is the reference field of 10 mT. The reduced attenuation of the coupled RSAW amplitude $\Delta P^{\rm norm}$ can be evaluated from S_{21} in a manner similar to that in the previous study [15, 30].

Figure 3(a) presents the color plot of $\Delta P^{\rm norm}$ as functions of frequency and external field for a device in which the width and spacing distance of the IDT finger electrode is 550 nm. The red dotted line shows the dispersion relation of the MSBVW, which can be given as [34, 35]

$$f = \frac{\gamma}{2\pi}\sqrt{|\mu_0 H|\left(|\mu_0 H| + \mu_0 M_s \frac{1-e^{-kd}}{kd}\right)}, \qquad (2)$$

where γ, k, d and M_s are the gyromagnetic ratio, wavenumber of the spin waves, thickness of the $Ni_{79}Fe_{21}$ film, and saturation magnetization, respectively. We use the following parameters for calculation: $\gamma = 1.86 \times 10^{11}$ $s^{-1}T^{-1}$, $k = 2.88 \times 10^6$ m^{-1}, $d = 20$ nm, and $\mu_0 M_s = 0.9$ T. Figure 3(b) shows the frequency variation with respect to the RSAW amplitude at 10 mT. Two peak intensities can be observed at frequencies in the range from 1.7 to 1.8 GHz, one of which corresponds to the excitation of RSAW which can couple with the MSBVW mode[36]. We observe the wave packet of RSAW from the time-domain S_{21} data and conclude that the sound velocity of the RSAW propagating through the $Ni_{79}Fe_{21}$ film is 3523 m/s. Based on the resonant frequency and sound velocity measured at 10 mT [36], the wavelength of the RSAW propagating through the $Ni_{79}Fe_{21}$ film is evaluated to be 2.0 μm; this is 8.5% shorter than wavelength measured for the sample without the $Ni_{79}Fe_{21}$ film whose value is consistent with the structural period of IDT. The reduced wavelength can be attributable to the difference in Poisson's ratio E and elastic modulus ν between the $LiNbO_3$ substrate and $Ni_{79}Fe_{21}$ film [37]. As shown in Fig. 3(a), the strongest microwave absorption can be observed when applying the resonant field at 1.75 GHz in the MSBVW mode. From a quantum-mechanical viewpoint, this is attributed to an avoided level crossing caused by a hybridization of the RSAW and MSBVW. The hybridized mode excited via magnetoelastic and gyromagnetic couplings can be distinguished based on the dependence of $\Delta P^{\rm norm}$ on the frequency and the angle of an external field [30]. From these experimental data, the magnetoelastically coupled RSAW could be ignored in case of the $Ni_{79}Fe_{21}$ film [36]. Figures 3(c) and 3(d) show the external field dependences of $\Delta P^{\rm norm}$ and $\Delta\theta$ at 1.75 GHz, respectively. Interestingly, in Fig. 3(d), a bipolar change in $\Delta\theta$ can be clearly observed in the vicinity of the avoided level crossing. Similar bipolar change was both numerically and experimentally observed in the magnetoelastically coupled RSAW [19, 38].

To discuss the origin of the bipolar change in $\Delta\theta$, we analytically solve the equation of motion for the $Ni_{79}Fe_{21}$ lattice by considering the EdH torque, which can be given as $\boldsymbol{\tau}^{\rm EdH} = -\gamma^{-1}\partial_t \boldsymbol{M}$. It is noted that the magneto-rotation coupling [11], which is also attributable to the interaction between acoustic and magnetic waves, can be neglected in the NiFe film because a perpendicular anisotropy is negligible in the NiFe film [36]. Moreover, if the magneto-rotation coupling coexists with the gyromagnetic coupling, a helical effective field, which leads to a nonreciprocal SWR excitation, is produced [36] although the SWR amplitude shows little change with switching the external field direction (Fig. 3(c)). The EdH torque contributes to the off-diagonal elements of an antisymmetric stress tensor [14]. It is convenient to discuss the longitudinal and transverse strain waves separately for quantitatively analyzing the EdH torque in RSAW because the conversion of angular momentum via EdH effect occurs between the magnetization and transverse strain waves. Finally, the velocity of the transverse strain wave modulated by the EdH effect can be evaluated. The RSAW velocity $c_{\rm R}$ can be given as $c_{\rm R} = \xi c_t$, where ξ is the velocity coefficient obtained by applying the stress condition on a free surface [36]. The RSAW velocity shift from $c_{\rm R}$ to $c'_{\rm R}$ because of the EdH effect can be evaluated from the change in the wavenumber of coupled RSAW, which is given as [36]

$$\Delta k = \frac{\omega}{c_{\rm R}} - \frac{\omega}{c'_{\rm R}} \approx \frac{\omega^3 \chi_{yy}}{4\rho\gamma^2\mu_0\xi c_{\rm t}^3} + \frac{\omega\Delta\xi c_t}{c_{\rm R}^2}. \qquad (3)$$

Here, ρ and χ_{yy} are the density of FM and (y, y) component of the Polder susceptibility tensor, respectively. $\Delta\xi$ represents the modulation of ξ owing to the EdH effect. When the surface displacement $\boldsymbol{u}$ of FM is described as $\boldsymbol{u} = \boldsymbol{u}_0 e^{i(kx-\omega t)}$,$\Delta\theta$ can be given as $L\Delta k$, where L is the propagating distance of the RSAW in FM. $\boldsymbol{u}_0$ has a constant value independent of both t and x. Figure 4 shows the calculated external field dependence of $\Delta\theta$. Here, we use the following parameters for calculation: $\omega = 2\pi \times 1.75$ GHz, $\rho = 8.70 \times 10^3$ kg/m^3, $c_{\rm t} = 3046$ m/s, and $L = 400$ μm [36, 39]. From Eq. (3), the magnetic field dependence of $\Delta\theta$ is expected to show antisymmetric Lorentzian variation according to the field variations in $\chi_{\rm yy}$ and $\Delta\xi$ [36]. However, in a practical device comprising FM with a finite lateral dimension, the temporal derivative of magnetization includes the off-diagonal component of the Polder susceptibility χ_{yz}. The field dependence of $\Delta\theta$ in Fig. 3(d) is well fitted by a combined function of symmetric and antisymmetric Lorentzian. The maximal phase shift $\Delta\theta_{\rm max}$ of -0.035 rad was observed at $\mu_0 H_{\rm ex} = 5.0$ mT, the order of magnitude of which is similar to the numerical result shown in Fig. 4, where a loss-less conversion of angular momentum is assumed between the spin and lattice systems. Thus, the consistency in $\Delta\theta$ suggests that the conversion efficiency of angular momentum with respect to the EdH effect is very high, as seen in Ref. [14]. Such an efficient conversion can be attributed to the fact that the EdH effect is a consequence of fundamental angular momentum conservation between electron spin and lattice rotation.

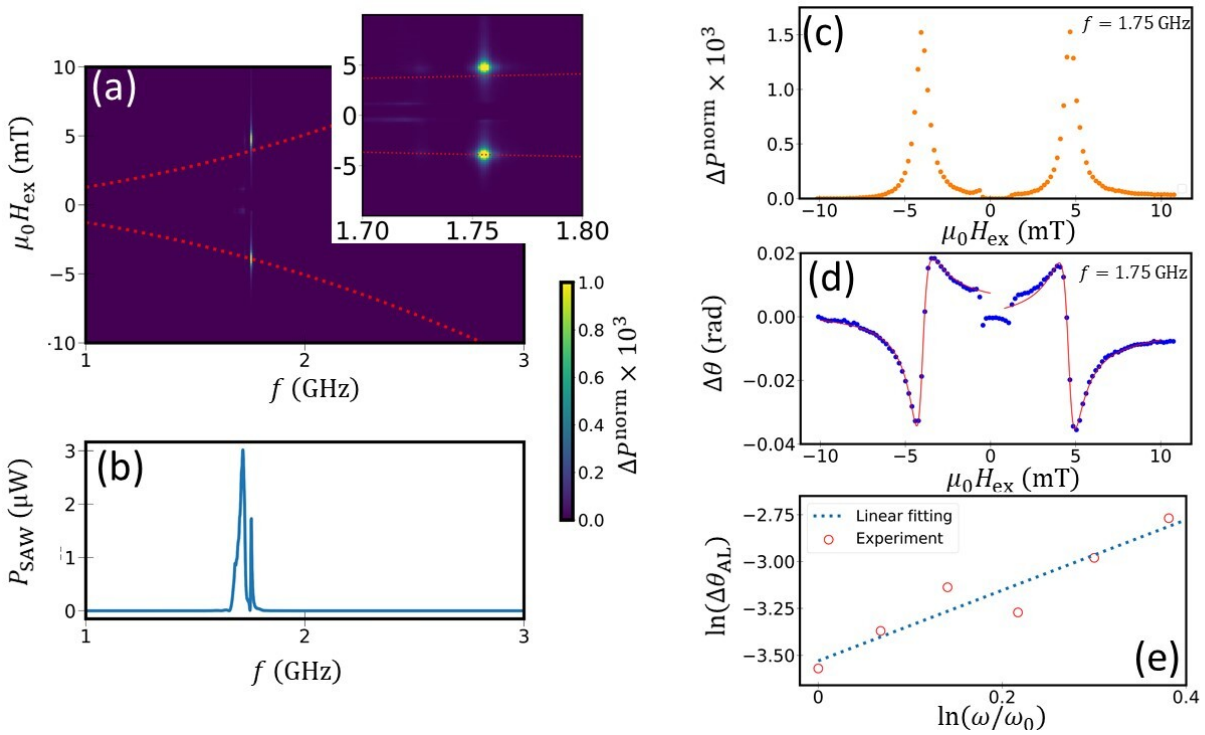

FIG. 3. (a) Color plot of $\Delta P^{\rm norm}$ as functions of frequency and external magnetic field. The red dotted line shows the MSBVW dispersion relation expected for the $Ni_{79}Fe_{21}(20)$ film. The inset shows the enlarged $\Delta P^{\rm norm}$ at frequencies of 1.70-1.80 GHz. (b) Transmitted microwave power as a function of frequency in the reference field $\mu_0 H_{\rm ref}$. (c) and (d) show $\Delta P^{\rm norm}$ and $\Delta\theta$ as a function of external field at the fundamental frequency of RSAW, i.e., 1.75 GHz. The red line shows the result of best fit with combined functions of symmetric and antisymmetric Lorentzian. (e) RSAW frequency dependence of $\Delta\theta_{\rm AL}$. The dotted line is the best-fit linear function to the data sets.

From the value of $\Delta\theta_{\rm max}$, the maximal Δk and $\Delta c_{\rm R}/c_{\rm R}$ are estimated to be 87 rad/m and 2.8×10^{-5}, respectively, where $\Delta c_{\rm R} = c'_{\rm R} - c_{\rm R}$. The value of $\Delta c_{\rm R}/c_{\rm R}$ in case of the EdH effect is comparable to that obtained in a previously conducted study that investigated the change in RSAW velocity in a Ni film owing to the magnetoelastic effect [20].

Figure 3(e) shows the double-logarithmic plot of $\Delta\theta_{\rm AL}$, which is the peak-to-peak amplitude of the anti-Lorentzian component of $\Delta\theta$ in Fig. 3(d) as a function of ω/ω_0, where ω_0 is $2\pi\times1.30$ GHz. The dotted line in Fig. 3(e) indicates best fit with a linear function, the slope of which is 1.88 ± 0.32. From Eq. (3), the amplitude of Δk, i.e., $\Delta\theta$, is expected to be proportional to the square of ω because χ_{yy} is inversely proportional to ω and $\Delta\xi$ is approximately proportional to ω [36]. The consistency in the frequency variation of $\Delta\theta$ suggests that the EdH phase shifts in the RSAW described by Eq. (3) occur because the phase shift owing to magentoelastic torque is proportional to ω [9, 33]. The higher-order variation of phase shift in case of EdH torque with respect to frequency indicates that the EdH torque would be dominated in terahertz regime as seem in Ref. [14] because we have observed the comparative phase shift in gigahertz regime.

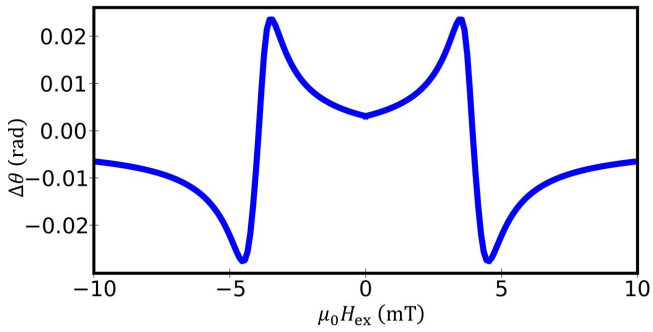

FIG. 4. External field dependence of the phase shift owing to the EdH effect estimated using Eq. (3).

In summary, we presented the phase shift of the RSAW based on the EdH effect in the $Ni_{79}Fe_{21}$ thin film. We considered an analytical model involving the magnetization dynamics induced by lattice rotation and elastic motion containing the stress that can be attributed to the EdH effect to discuss the origin of the phase shift quantitatively. By comparing the experimental and numerical results, we observed that the magnitude and frequency variations of phase shift can be quantitatively explained

based on the assumption that the conversion of angular momentum between electron spin and lattice systems is ideally adiabatic. In the gigahertz regime, we observed that the maximum ratio of velocity change was comparable to that observed in the case in which the magnetoelastic effect was considered. Moreover, compared with the case in which magnetoelastic torque was considered, the order of variation in phase shift with respect to frequency increased in the case in which EdH torque was considered. From an application viewpoint, the EdH torque is more feasible for high speed spin-based RSAW devices.

The authors would like to thank J. Fujimoto for his valuable discussions. This work was partially supported by JSPS KAKENHI Grant NO. JP18H03867 and JST CREST Grant Number JPMJCR19J4, Japan.

[1] A. Einstein and W. J. de Haas, Experimenteller Nachweis der Ampreschen Molekularstrme. Verhandl. Deut. Phys. Ges. 17, 152170 (1915).

[2] F. W. Hehl and W. T. Ni, Inertial effects of a Dirac particle, Phys. Rev. D **42**, 2045 (1990).

[3] J. Frlich and U. M. Studer, Gauge invariance and current algebra in nonrelativistic many-body theory, Rev. Mod. Phys. **65**, 733, (1993)

[4] M. Matsuo, J. Ieda, E. Saitoh, and S. Maekawa, Effects of mechanical rotation on spin currents, Phys. Rev. Lett. **106**, 076601 (2011).

[5] M. Matsuo, J. Ieda, K. Harii, E. Saitoh, and S. Maekawa, Mechanical generation of spin current by spin-rotation coupling, Phys. Rev. B **87**, 180402(R) (2013).

[6] M. Matsuo, Y. Ohnuma, and S. Maekawa, Theory of spin hydrodynamic generation, Physical Review B 96, 020401(R)(2017).

[7] M. Weiler, L. Dreher, C. Heeg, H. Huebl, R. Gross, M.S. Brandt, and S.T.B. Goennenwein, Elastically Driven Ferromagnetic Resonance in Nickel Thin Films, Phys. Rev. Lett. **106**, 117601 (2011).

[8] M. Weiler, H. Huebl, F. S. Goerg, F. D. Czeschka, R. Gross, and S. T. B. Goennenwein, Spin Pumping with Coherent Elastic Waves, Phys. Rev. Lett. **108**, 176601 (2012).

[9] L. Dreher, M. Weiler, M. Perpeintner, H. Huebl, R. Gross, M. S. Brandt, and S. T. B. Goennenwein, Surface acoustic wave driven ferromagnetic resonance in nickel thin films: Theory and experiment, Phys. Rev. B **86** 134415 (2012).

[10] M. Xu, J. Puebla, F. Auvray, B. Rana, K. Kondou, and Y. Otani, Inverse Edelstein effect induced by magnon-phonon coupling, Phys. Rev. B **97**, 180301 (R) (2018).

[11] M. Xu, K. Yamamoto, J. Puebla, K. Baumgaertl, B. Rana, K. Miura, H. Takahashi, D. Grundler, S. Maekawa, and Y. Otani, Nonreciprocal surface acoustic wave propagation via magneto-rotation coupling, Sci. Adv **6**, 1724-1∼4 (2020).

[12] K. Harii, Y. Seo, Y. Tsutsumi, H. Chudo, K. Oyanagi, M. Matsuo, Y. Shiomi, T. Ono, S. Maekawa, and E. Saitoh, Spin Seebeck mechanical force, Nat. Commun. **10**, 2616 (2019).

[13] K. Mori, M. G. Dunsmore, J. E. Losby, D. M. Jenson, M. Belov, and M. R. Freeman, Einsteinde Haas effect at radio frequencies in and near magnetic equilibrium, Phys. Rev. B **102**, 054415 (2020).

[14] C. Dornes, Y. Acremann, M. Savoini, M. Kubli, M. J. Neugebauer, E. Abreu, L. Huber, G. Lantz, C. A. F. Vaz, H. Lemke, E. M. Bothschafter, M. Porer, V. Esposito, L. Rettig, M. Buzzi, A. Alberca, Y. W. Windsor, P. Beaud, U. Staub, D. Zhu, S. Song, J. M. Glownia, and S. L. Johnson, The ultrafast Einstein-de Haas effect, Nature (London) **565**, 209 (2019).

[15] D. Kobayashi, T. Yoshikawa, M. Matsuo, R. Iguchi, S. Maekawa, E. Saitoh, and Y. Nozaki, Spin Current Generation Using a Surface Acoustic Wave Generated via Spin-Rotation Coupling, Phys. Rev. Lett **119**, 077202 (2017).

[16] S. Tateno, G. Okano, M. Matsuo, and Y. Nozaki, Electrical evaluation of the alternating spin current generated via spin-vorticity coupling, Phys. Rev. B **102**, 104406 (2020).

[17] Y. Kurimune, M. Matsuo, S. Maekawa, and Y. Nozaki, Highly nonlinear frequency-dependent spin-wave resonance excited via spin-vorticity coupling, Phys. Rev. B **102**, 174413 (2020).

[18] T. Kawada, M. Kawaguchi, T. Funato, H. Kohno, M. Hayashi, Acoustic spin Hall effect in strong spin-orbit metals, Sci. Adv. **7**, eabd9697 (2021).

[19] J.-Y. Duquesne, P. Rovillain, C. Hepburn, M. Eddrief, P. Atkinson, A. Anane, R. Ranchal, and M. Marangolo, Surface-Acoustic-Wave Induced Ferromagnetic Resonance in Fe Thin Films and Magnetic Field Sensing, Phys. Rev. Applied **12**, 024042 (2019).

[20] R. Sasaki, Y. Nii, Y. Iguchi, and Y. Onose, Nonreciprocal propagation of surface acoustic wave in Ni/$LiNbO_3$, Phys. Rev. B **95**, 020407(R). (2017).

[21] S. Tateno and Y. Nozaki, Highly Nonreciprocal Spin Waves Excited by Magnetoelastic Coupling in a Ni/S Bilayer, Phys. Rev. Applied **13** 034074 (2020).

[22] A. Hernndez-Mnguez, F. Maci, J. M. Hernndez, J. Herfort, and P. V. Santos, Large Nonreciprocal Propagation of Surface Acoustic Waves in Epitaxial Ferromagnetic/Semiconductor Hybrid Structures, Phys. Rev. Applied **13**, 044018 (2020).

[23] R. Verba, I. Lisenkov, I. Krivorotov, V. Tiberkevich, and A. Slavin, Nonreciprocal Surface Acoustic Waves in Multilayers with Magnetoelastic and Interfacial Dzyaloshinskii-Moriya Interactions, Phys. Rev. Applied **9**, 064014 (2018).

[24] R. Verba, V. Tiberkevich, and A. Slavin, Wide-Band Nonreciprocity of Surface Acoustic Waves Induced by Magnetoelastic Coupling with a Synthetic Antiferromagnet, Phys. Rev. Applied **12**, 054061 (2019).

[25] M. K, M. Heigl, L. Flacke, A. Hrner, M. Weiler, M. Albrecht, and A. Wixforth, Nonreciprocal DzyaloshinskiiMoriya Magnetoacoustic Waves,Phys. Rev. Lett. **125**, 217203 (2020).

[26] P. J. Shah, D. A. Bas, I. Lisenkov, A. Matyushov, N. X. Sun, and M. R. Page, Giant nonreciprocity of surface acoustic waves enabled by the magnetoelastic interaction, Sci. Adv. **6**, 49, eabc5648 (2020).

[27] M. K, M. Heigl, L. Flacke, A. Hrner, M. Weiler, A. Wixforth, and M. Albrecht, Nonreciprocal Magnetoacoustic Waves in Dipolar-Coupled Ferromagnetic Bilayers, Phys.

Rev. Applied **15**, 034060 (2021).
[28] L. Thevenard, I. S. Camara, S. Majrab, M. Bernard, P. Rovillain, A. Lemaitre, C. Gourdon, and J.-Y. Duquesne, Precessional magnetization switching by a surface acoustic wave, Phys. Rev. B **93**, 134430 (2016).
[29] W. A. Misba, M. M. Rajib, D. Bhattacharya, and J. Atulasimha, Acoustic-Wave-Induced Ferromagnetic-Resonance-Assisted Spin-Torque Switching of Perpendicular Magnetic Tunnel Junctions with Anisotropy Variation, Phys. Rev. Applied **14**, 014088 (2020).
[30] Y. Kurimune, M. Matsuo, and Y. Nozaki, Observation of Gyromagnetic Spin Wave Resonance in $Ni_{79}Fe_{21}$ Films, Phys. Rev. Lett. **124**, 217205 (2020).
[31] S. J. Barnett, Magnetization by Rotation, Phys. Rev. **6**, 239 (1915).
[32] S. J. Barnett, Gyromagnetic and Electron-Inertia Effects, Rev. Mod. Phys. **7**, 129 (1935).
[33] P. G. Gowtham, D. Labanowski, and S. Salahuddin, Mechanical back-action of a spin-wave resonance in a magnetoelastic thin film on a surface acoustic wave, Phys. Rev. B **94**, 014436 (2016).
[34] D. D. Stancil and Prabhakar, *Spin Waves : Theory and Application* (Springer, New York, 2009).
[35] B. A. Kalinikos, Excitation of propagating spin waves in ferromagnetic films, IEE Proc. **127**, 4 (1980).
[36] See supplemental information at ***
[37] H. F. Tiersten, Elastic Surface Waves Guided by Thin Films, J. Appl. Phys., **40**, 770 (1969).
[38] L. Thevenard, C. Gourdon, J. Y. Prieur, H. J. von Bardeleben, S. Vincent, L. Becerra, L. Largeau, and J.-Y. Duquesne, Surface-acoustic-wave-driven ferromagnetic resonance in (Ga,Mn)(As,P) epilayers, Phys. Rev. B **90**, 094401 (2014).
[39] For the material parameters of $Ni_{79}Fe_{21}$ film, ρ, c_t, c_l, we used a liner complemented value from bulk Ni and Fe according to the alloy ratio.